Wavelet-driven Decoupling and Physics-informed Mapping Network for Accelerated Multi-parametric MR Imaging

Ruilong Dan[1], Kaicong Sun[1(✉)], Yichen Zhou[1], Minqiang Jia[1], Yuxuan Liu[1], Han Zhang[1], Xiaopeng Zong[1], Dinggang Shen[1,2,3(✉)]

[1] School of Biomedical Engineering & State Key Laboratory of Advanced Medical Materials and Devices, ShanghaiTech University, Shanghai 201210, China
sunkc@shanghaitech.edu.cn, Dinggang.Shen@gmail.com
[2] Shanghai United Imaging Intelligence Co., Ltd., Shanghai 200230, China
[3] Shanghai Clinical Research and Trial Center, Shanghai, 201210, China.

Abstract. Multi-parametric magnetic resonance imaging (MRI) is an advanced MRI technique that can provide multiple quantitative maps simultaneously based on acquired multi-echo images. However, the lengthy scan time often limits its application. Accelerated multi-parametric MRI using deep learning is of great interest. The existing studies have two limitations: 1) inefficient use of the multi-echo information; 2) lack of physical prior for parametric mapping. To address these issues, in this work, we propose a novel decoupling-driven and physics-informed reconstruction network for accelerated multi-parametric MRI. Specifically, to better align and integrate multi-echo information, we propose a novel decoupling technique consisting of wavelet-driven decoupling module, contrastive and echo-dependent decoupling losses, such that the multi-echo features can be effectively decoupled into echo-dependent and echo-independent components. Only the echo-independent features are fused across multiple echoes. Besides, Bloch equations are incorporated as physical priors to guide the parametric mapping network. Experimental results on our in-house data (12-echo sequence) show that our method outperforms the state-of-the-art methods by 1.54% in average SSIM and 1.70dB in average PSNR for 4× acceleration, which significantly advances the performance limitation for multi-parametric MRI. Our code is available at https://github.com/IDEARL23/WDPM-Net.

Keywords: Multi-parametric MRI · Quantitative MRI · Wavelet-driven · Feature decoupling · Physics-informed mapping.

1 Introduction

Multi-parametric magnetic resonance imaging (MRI) is an advanced MRI technique that can provide intrinsic tissue properties like proton density (PD), T_1 map, and T_2^* map simultaneously through a single scan [11, 22] and is safer than the radioactive imaging modalities, such as computed tomograph (CT)

and positron emission tomography (PET) [5]. However, the multi-echo nature of the acquisition sequence results in prolonged scan times, thereby highlighting the importance of accelerated acquisition in multi-parametric MRI.

Multi-parametric MRI pipelines usually contain two separate steps: multi-echo image reconstruction from under-sampled k-space data and desired maps or images estimation via signal modeling [4,22,23]. Current deep learning-based approaches for multi-parametric MR imaging mainly fall into two categories: (1) Two-step methods [2,24] and (2) One-step methods [1,6,9]. The former one first reconstructs multi-echo images from undersampled k-space [7,8], and then estimates parametric maps via empirical physical models [4,22,23]. Such framework suffers from error propagation due to the remaining artifacts left in the reconstructed images in step one. The latter one like MANTIS [9] directly maps k-space to parametric maps via unified networks, yet ignores intermediate supervision on the reconstructed images. The recent work SRM-Net [11] attempts joint optimization of the reconstruction and mapping networks. Although they have achieved noticeable performance improvement, they still have two main limitations: (1) the highly-coupled multi-echo information is inadequately exploited; and (2) no physical prior is integrated for parametric mapping. In summary, both categories struggle to balance multi-echo synergy, physics constraints, and co-optimization, highlighting unmet needs for effective multi-echo feature interaction mechanisms and physically constrained mapping architectures.

To this end, we introduce a novel Wavelet-driven Decoupling and Physics-informed Mapping Network (WDPM-Net) designed for efficient multi-echo feature interaction and physics-guided parametric mapping. ***First***, we decouple the echo-independent features (e.g., anatomical structures) from the echo-dependent features (e.g., contrast) by adaptively weighed wavelet transformation and two elaborately designed decoupling losses. The echo-independent features are aligned and fused to form consensus for robust reconstruction. ***Second***, we introduce a physics-informed mapping network (PIMN) by integrating analytically estimated maps as prior to guide the mapping network, ensuring more accurate and reliable parametric mapping. In summary, our contributions are mainly four-fold:

1. We propose a novel Decoupling-driven and Physics-informed Reconstruction Network (WDPM-Net) for accelerated multi-parametric MRI, effectively addressing the limitations of inefficient multi-echo exploration and overlooking of physical priors in deep learning-based multi-parametric MRI.
2. We introduce an effective feature decoupling scheme including dedicated Wavelet-driven network and elaborately designed contrastive and echo-dependent consistency losses, which enables more efficient multi-echo integration.
3. We have developed the first physics-informed parametric mapping network by combining data-driven prediction with physics-driven Bloch equations, improving the robustness and fidelity of the estimated parametric maps.
4. Experimental results on our in-house dataset (12-echo sequence) demonstrate that our method outperforms the state-of-the-art methods by 1.54% in average SSIM and 1.70dB in average PSNR for 4× acceleration, significantly advancing the performance limitation for multi-parametric MRI.

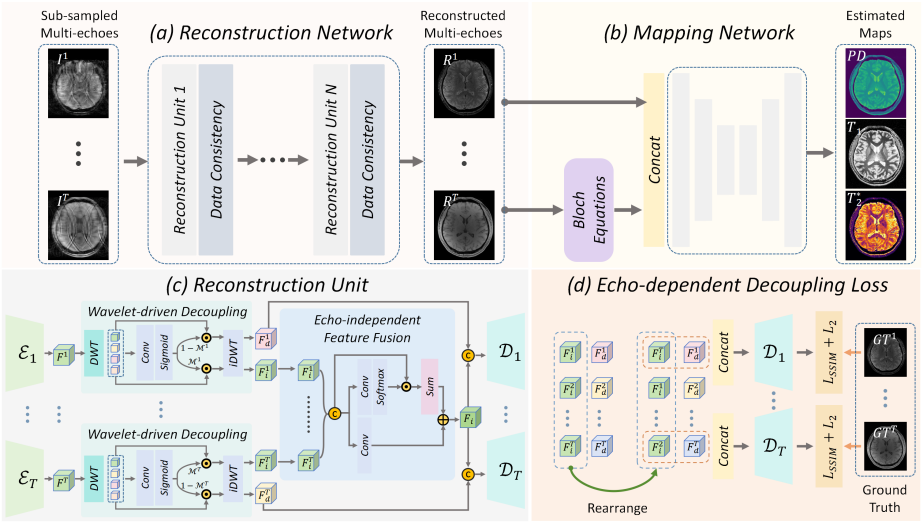

Fig. 1. The overall framework of the proposed WDPM-Net with (a) multi-echo reconstruction, (b) physics-informed parametric mapping in an end-to-end manner to accelerate multi-parametric MRI, (c) details of the reconstruction unit (RU), and (d) details of the echo-dependent decoupling loss. The reconstruction network consists of cascaded RUs, containing wavelet-driven decoupling and echo-independent feature fusion modules, to refine multi-echo MR reconstruction. The mapping network estimates the maps based on the reconstructed images under the guidance of Bloch equations.

2 Method

2.1 Overview of the Proposed Framework

Our framework comprises two main parts: (a) a multi-echo reconstruction network and (b) a parametric mapping network as shown in Fig. 1. The multi-echo reconstruction network consists of cascaded reconstruction units (RU) followed by a data consistency layer to reconstruct and refine the multi-echo images. Based on this, the physics-informed parametric mapping network generates the quantitative maps under the guidance of the initial estimation from multi-dimensional integration (MDI) and Bloch equations [22].

2.2 Wavelet-driven Feature Decoupling and Fusion

Wavelet-driven Decoupling Module. Feature decoupling aims to separate features into varied parts to finely control the information sharing adhered to domain priors and has presented promising performance in multi-modal feature fusion in MRI analysis [8, 10, 13, 14]. Though there were attempts to disentangle features for MR reconstruction, their performance is limited by insufficient decoupling [14, 21] or hand-crafted separation [15]. Moreover, some

works [15, 17, 19, 20] were tailored to two contrasts thus hard to extend to complex scenarios such as multi-echo reconstruction. In this work, we employ wavelet transforms to decompose features into approximation (LL) and detail (LH, HL, HH) subbands, facilitating decoupling of different frequency components inherent in the features. By applying a spatial attention mechanism in the wavelet domain, we can adaptively emphasize the echo-independent features in an adaptive manner. Specifically, for each echo t, corresponding extracted features F^t are transformed into wavelet subbands $F_w^t \in \mathcal{R}^{C\times\frac{H}{2}\times\frac{W}{2}}$ via discrete haar wavelet transform (DWT). Spatial attention maps $\mathcal{M}^t \in [0,1]^{4C\times\frac{H}{2}\times\frac{W}{2}}$, generated by a convolution layer and a sigmoid layer, split F_w^t into echo-independent feature F_i^t and echo-dependent feature F_d^t in the wavelet domain by Eq. (1), where $\odot$ denotes the Hadamard product and iDWT denotes the inverse DWT.

$$F_i^t = \text{iDWT}(\mathcal{M}^t \odot F_w^t), \quad F_d^t = \text{iDWT}((1-\mathcal{M}^t) \odot F_w^t) \tag{1}$$

Echo-independent Feature Fusion. To obtain robust and consistent reconstruction across multi-echo images, we fuse echo-independent features $\{F_i^1, \ldots, F_i^T\}$ from T echoes. Specifically, we design a feature fusion module that adaptively fuses spatial structures across multiple echos. First, all features are concatenated and then processed by a convolutional layer to generate T spatial attention maps $\{\alpha^t\}_{t=1}^T$. These T maps are then normalized via softmax along the channel to adaptively weight the contribution of each echo's anatomical features. The weighted features are summed to produce an initial fused feature F_i^{init}, while a residual connection through a 1×1 convolution is added to F_i^{init}, yielding the final fused feature F_i that preserves consistent anatomical structures. The processes are formulated in Eq. (2) and (3).

$$\{\alpha^t\}_{t=1}^T = \text{Softmax}\left(\text{Conv}\left(\text{Channel Concat}(F_i^1, F_i^2, \ldots, F_i^T)\right)\right) \tag{2}$$

$$F_i = \text{Conv}_{1\times1}\left(\text{Channel Concat}(F_i^1, F_i^2, \ldots, F_i^T)\right) + \sum_{t=1}^{T} \alpha^t \odot F_i^t \tag{3}$$

Echo-dependent Decoupling Loss. To preserve the echo-dependent information of each echo image, e.g., contrast information, we propose an echo-dependent decoupling (ED) loss as depicted in Fig. 1 (d). Specifically, the ED loss randomly rearranges the echo-independent features (i.e., F_i^1 to F_i^T) and constructs new T paired combinations. The re-ordered combinations are enforced to generate the same image as the corresponding ground-truth (GT) image. It is worth noting that our proposed ED loss has great scalability and can be extended to arbitrary amount of echo images. The ED loss is expressed as Eq. (4), where $\hat{I}^t$ is the t-th reconstructed echo image with λ_1 being a tunable hyperparameter.

$$\mathcal{L}_{\text{ED}} = \sum_{t=1}^{T} [\|\hat{I}^t - \text{GT}^t\|_2 + \lambda_1 L_{\text{SSIM}}(\hat{I}^t, \text{GT}^t)], \tag{4}$$

Contrastive Decoupling Loss. To explicitly perform decoupling and alignment for efficient fusion, a contrastive decoupling (CD) loss is designed to cluster the echo-independent features $\{F_i^t\}_{t=1}^T$ (i.e., positive pairs) and push the

echo-dependent features $\{F_d^t\}_{t=1}^T$ apart (i.e., negative pairs). Specifically, all the $\{F_d^t\}_{t=1}^T$ and $\{F_i^t\}_{t=1}^T$ as well as the fused feature F_i are first flattened and normalized with L_2 norm. Thanks to the CD loss, we can regularize the feature space according to MR imaging priors, facilitating the decoupling between echo-independent and echo-dependent features while promoting alignment across echo-independent features. The total CD loss can be expressed as:

$$\mathcal{L}_{\text{CD}} = \frac{1}{T(T-1)} \sum_{p \neq q} \cos(F_d^p, F_d^q) + \frac{1}{T} \sum_{t=1}^{T} \cos(F_i^t, F_d^t) - \frac{1}{T} \sum_{t=1}^{T} \cos(F_i^t, F_i) \quad (5)$$

2.3 Physics-informed Network for Multi-parametric Mapping

Traditional parametric mapping is usually performed by Bloch equations, which are highly sensitive to the quality and fidelity of the reconstructed multi-echo MR images [11, 22] and hinders the end-to-end optimization of reconstruction and mapping. Though there were attempts [11] introducing MLPs to imitate nonlinear mapping, the mapping performance is limited by the learning capacity of MLPs. In this work, we propose to apply more powerful network and integrate physical priors from Bloch equations [22] to improve the mapping performance.

Bloch Equation-based Multi-parametric Mapping. The initial estimation of T_1 map ($\mathrm{T}_1|_{\text{init}}$) and T_2^* map ($\mathrm{T}_2^*|_{\text{init}}$) can be calculated by Eq. (6), where TR_N ($N \in \{1, 2\}$) is the repetition time. k is a physical parameter corresponding to repetition time, flip angle, and the acquired MR signal. $\mathrm{B}_{1\mathrm{t}}$ is the transmission radio frequency field, $\Delta\mathrm{TE}$ is the difference of the echo times and ΔS is the corresponding signal difference. The above required parameters can be determined analytically. More details can be found in [22].

$$\mathrm{T}_1|_{\mathrm{TR}_N} = \frac{\mathrm{TR}_1}{|k_{\mathrm{TR}_N}| \cdot \mathrm{B}_{1\mathrm{t}}}, \quad \mathrm{T}_1|_{\text{init}} = \frac{\mathrm{T}_1|_{\mathrm{TR}_1} + \mathrm{T}_1|_{\mathrm{TR}_2}}{2}, \quad \mathrm{T}_2^*|_{\text{init}} = \frac{-\Delta\mathrm{TE}}{\ln|\Delta S|} \quad (6)$$

Physics-informed Mapping Network. Based on the reconstructed echo images and Eqs. (6), we can yield the initial estimation of the maps $\mathbf{P}_{\text{init}} = \{\mathrm{T}_1|_{\text{init}}, \mathrm{T}_2^*|_{\text{init}}\}$ by multi-echo fitting. These initial maps are concatenated with the reconstructed echo images $\mathbf{I}_{\text{init}} = \{I_{\text{init}}^t\}_{t=1}^T$ and processed by a UNet [16] as shown in Fig. 1 (b). In this way, our PIMN bridges data-driven learning and physics-informed constraints for multi-parametric MRI, resulting in more robust and physically plausible mapping than solely data-driven or physics-driven estimations. Moreover, we can easily combine the PIMN with off-the-shelf multi-echo reconstruction methods for multi-parametric mapping as demonstrated in the experiments.

2.4 Loss Function

The total loss consists of three parts, including the multi-echo reconstruction loss in Eq. (7), feature decoupling loss in Eq. (8), and multi-parametric mapping

loss in Eq. (9). We train our method in an end-to-end fashion, thus the total loss is summarized as Eq. (10), where λ_1, λ_2, λ_3, and λ_4 denote hyper-parameters used to balanced different losses, and are empirically set to 0.5, 1, 0.1, and 2, respectively.

$$\mathcal{L}_{\text{Recon}} = \|\mathbf{I}_{\text{final}} - \mathbf{I}_{\text{GT}}\|_2 + \lambda_1 L_{\text{SSIM}}(\mathbf{I}_{\text{final}}, \mathbf{I}_{\text{GT}}) \tag{7}$$

$$\mathcal{L}_{\text{Decouple}} = \mathcal{L}_{\text{ED}} + \lambda_2 \mathcal{L}_{\text{CD}} \tag{8}$$

$$\mathcal{L}_{\text{Map}} = \|\mathbf{P}_{\text{final}} - \mathbf{P}_{\text{GT}}\|_2 + \lambda_1 L_{\text{SSIM}}(\mathbf{P}_{\text{final}}, \mathbf{P}_{\text{GT}}) \tag{9}$$

$$\mathcal{L}_{\text{total}} = \mathcal{L}_{\text{Recon}} + \lambda_3 \mathcal{L}_{\text{Decoupling}} + \lambda_4 \mathcal{L}_{\text{map}} \tag{10}$$

3 Experiments

Dataset and Implementation Details. We evaluated our model on an in-house complex-valued dataset acquired by MULTIPLEX (MTP) [22] based on a 3T scanner (uMR 890). The MTP is a gradient echo pulse sequence (GRE) with following scanning parameters: FA_1/ FA_2=4°/16°, TR_1/TR_2=37.2 ms / 40 ms, and six echo images per FA with TR_1 (TE=3.86 ms) and TR_2 (TE=3.86/ 8.95/ 14.04/ 19.13/ 24.22 ms). Specifically, our dataset includes 42 subjects, with 12 echos per subject. The MRI scanning was based on a 64-channel head coil with a voxel size of $0.823 \times 0.823 \times 2\text{mm}^3$ and slice matrix size of $231 \times 272 \times 64$. To balance computation cost and reconstruction efficiency, we center-cropped the slices into 224×256 (50 slices per subject). The ground truth multi-coil multi-echo images and parametric maps are from vendor software. Our model inputs the coil-combined data using sensitivity maps calculated by ESPIRIT [18]. The 42 subjects were randomly split into subsets of 28, 4, and 10 subjects, corresponding to 1400, 200, and 500 slices for training, validation, and testing, respectively. To quantitatively assess performance, the following experiments apply two widely-used evaluation metrics, SSIM and PSNR. All our experiments were based on NVIDIA A100 GPUs (with 80GB RAM) and the Pytorch framework. Moreover, we applied the AdamW optimizer and trained the model for 300 epochs with mini-batch size set to 2 and learning rate set to 1×10^{-3}. In this work, we utilized the encoder $\mathcal{E}$ and decoder $\mathcal{D}$ from MIMOUNet [3,12] to extract multi-stage features and applied our WD module in each stage. Given the trade-off between training efficiency and reconstruction accuracy, RU's cascaded number N was set to 2.

Quantitative Comparison with State-of-the-Art Methods. Two representative MRI reconstruction methods are compared, including MANTIS [9] and SRM-Net [11]. Also, to assess the generalization capacity of our method, we extend a state-of-the-art (SOTA) multi-echo reconstruction method, JUST-Net [7], with our PIMN. The quantitative comparison with the existing SOTA methods on our dataset is summarized in Table 1, where our WDPM-Net consistently presents promising SSIM and PSNR under varied accelerating factors. For instance, our WDPM-Net outperforms the second best JUST-Net [7] by 3.62% in SSIM, for 4× acceleration. These quantitative results on varied AFs demonstrate

Table 1. Performance comparison of our model with existing methods on the dataset with equispaced sampling masks. The best results are in **bold**. AF: acceleration factor.

AF	Method	Reconstruction		PD		T1		T2*		Mapping	
		SSIM	PSNR	SSIM	PSNR	SSIM	PSNR	SSIM	PSNR	SSIM	PSNR
×4	Zero Filling	0.5425	23.72	-	-	-	-	-	-	-	-
	MANTIS [9]	-	-	0.7092	22.74	0.7629	27.20	0.9005	30.98	0.7909	26.97
	SRM-Net [11]	0.8548	31.26	0.8153	22.96	0.7405	26.72	0.9047	31.46	0.8201	27.05
	JUST-Net [7]	0.9157	32.67	0.8575	23.32	0.7785	27.32	0.8790	28.76	0.8383	26.47
	Ours	**0.9311**	**34.37**	**0.8990**	**24.08**	**0.8088**	**28.34**	**0.9157**	**31.46**	**0.8745**	**27.96**
×8	Zero Filling	0.4424	20.97	-	-	-	-	-	-	-	-
	MANTIS [9]	-	-	0.6827	20.90	0.7061	25.80	0.8821	29.59	0.7570	25.43
	SRM-Net [11]	0.8316	30.48	0.7979	22.06	0.7286	26.36	**0.8992**	**31.20**	0.8086	26.54
	JUST-Net [7]	0.8584	29.24	0.8329	22.63	0.7409	26.26	0.8630	29.58	0.8123	26.16
	Ours	**0.8766**	**30.57**	**0.8586**	**23.51**	**0.7566**	**27.07**	0.8939	29.95	**0.8364**	**26.84**

that our WDPM-Net outperforms the existing benchmark methods significantly, which is highly attributed to the efficacy of our proposed decoupling-driven reconstruction and physics-informed mapping framework. Also, the performance of the JUST-Net equipped with our PIMN demonstrates the desired plug-and-play attributes of our PIMN.

Qualitative Comparison with State-of-the-Art Methods. Furthermore, we visually compared the investigated methods on the testing dataset and illustrated the results in Fig. 2. The first row presents the GT and the reconstructed images using different methods. The second row shows the corresponding error maps, and the third row shows the zoom-in views of the ROI. From the error maps, we can see that our method performs best among all the comparison methods on both multi-echo reconstruction and parametric mapping, respectively. Particularly, as evident in the regions pointed out by the yellow arrows, our reconstructed images contain more detailed and clearer tissue structures as the zoom-in views depict. Visual inspection coincides with the quantitative measures, revealing the clinical potential of our method.

Table 2. Ablation study with 4× acceleration and equispaced sampling for the three main components of our WDPM-Net, including the WD module, decoupling loss, and physics-informed mapping.

WD Module	Decoupling loss	Physics-Informed	Reconstruction		Mapping	
			SSIM	PSNR	SSIM	PSNR
			0.8942	33.13	0.8074	26.92
✓			0.9281	34.16	0.8379	27.30
✓	✓		0.9300	34.27	0.8570	27.69
✓	✓	✓	**0.9311**	**34.37**	**0.8745**	**27.96**

Ablation Study. In this section, we evaluated the efficacy of the three key components in WDPM-Net by gradually adding the components. The experimental results are in Table 2, where the models equipped with all components

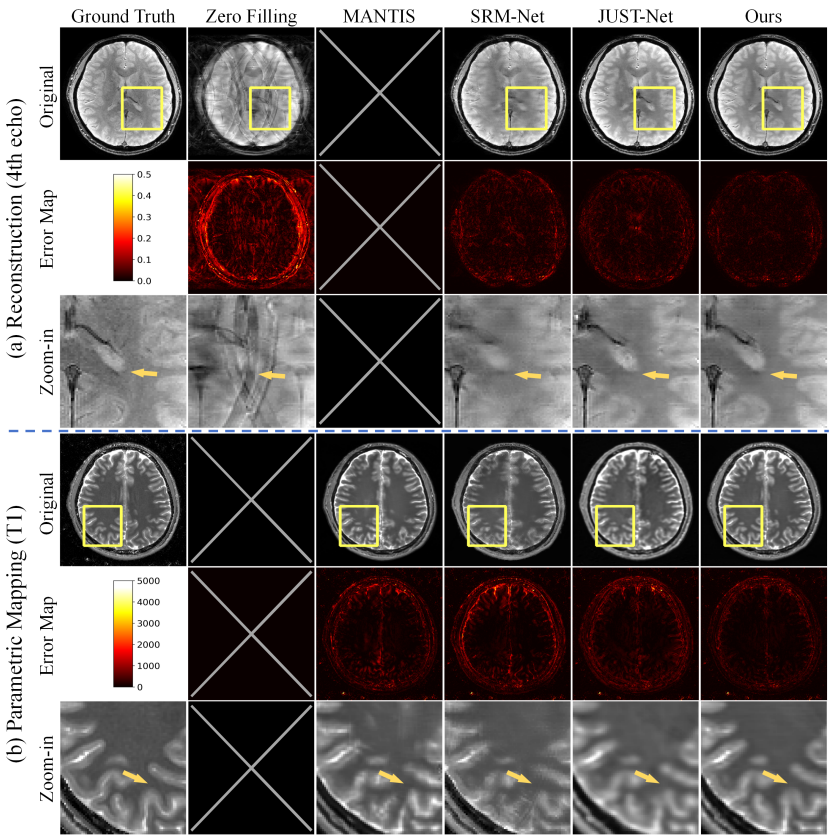

Fig. 2. Visual comparison of different methods on the test data with 4× equispaced sampling. The yellow boxes are shown in close-up views, and the reconstruction error maps of different methods are highlighted by the yellow arrows. The cross symbols indicate unavailable results.

perform the best, indicating that the components can collaboratively enhance overall reconstruction and mapping performance.

4 Conclusion

In this paper, we have presented WDPM-Net, a novel decoupling-driven and physics-informed mapping network. Different from the existing multi-parametric mapping methods, we propose to decouple the features of multi-echo images into echo-independent and echo-dependent ones by a novel Wavelet-driven network and also elaborately designed decoupling losses. Thus, multi-echo information can be more efficiently exploited and fused. Furthermore, we propose to integrate Bloch equation as physical priors into the multi-parametric mapping network, which enhances the mapping robustness and reliability. Experimental

results on our in-house dataset demonstrate that our method outperforms the state-of-the-art methods quantitatively and qualitatively, establishing a promising benchmark for accelerated multi-parametric MRI.

Acknowledgments. This work was supported in part by National Natural Science Foundation of China (grant numbers 82441023, U23A20295, 62131015, 62301318, 82394432), the China Ministry of Science and Technology (S20240085, STI2030-Major Projects-2022ZD0209000, STI2030-Major Projects-2022ZD0213100), Shanghai Municipal Central Guided Local Science and Technology Development Fund (No. YDZX20233100001001), The Key R&D Program of Guangdong Province, China (grant number 2023B0303040001), and HPC Platform of ShanghaiTech University.

Disclosure of Interests. The authors declare that they have no conflict of interest.

References

1. Cai, C., et al.: Single-shot t2 mapping using overlapping-echo detachment planar imaging and a deep convolutional neural network. Magnetic Resonance in Medicine **80**(5), 2202–2214 (2018)
2. Chaudhari, A., Fang, Z., Hyung Lee, J., Gold, G., Hargreaves, B.: Deep learning super-resolution enables rapid simultaneous morphological and quantitative magnetic resonance imaging. In: Machine Learning for Medical Image Reconstruction: First International Workshop, MLMIR 2018, Held in Conjunction with MICCAI 2018, Granada, Spain, September 16, 2018, Proceedings. pp. 3–11. Springer (2018)
3. Cho, S.J., Ji, S.W., Hong, J.P., Jung, S.W., Ko, S.J.: Rethinking coarse-to-fine approach in single image deblurring. In: Proceedings of the IEEE/CVF International Conference on Computer Vision. pp. 4641–4650 (2021)
4. Cordes, D., Yang, Z., Zhuang, X., Sreenivasan, K., Mishra, V., Hua, L.H.: A new algebraic method for quantitative proton density mapping using multi-channel coil data. Medical Image Analysis **40**, 154–171 (2017)
5. Huang, H., et al.: Metaad: Metabolism-aware anomaly detection for parkinson's disease in 3d 18 f-fdg pet. In: Medical Image Computing and Computer-Assisted Intervention – MICCAI. pp. 291–301. Springer (2024)
6. Jun, Y., Shin, H., Eo, T., Kim, T., Hwang, D.: Deep model-based magnetic resonance parameter mapping network (dopamine) for fast t1 mapping using variable flip angle method. Medical Image Analysis **70**, 102017 (2021)
7. Lee, J.H., et al.: Just-net: Jointly unrolled cross-domain optimization based spatio-temporal reconstruction network for accelerated 3d myelin water imaging. Magnetic Resonance in Medicine **91**(6), 2483–2497 (2024)
8. Lei, P., Fang, F., Zhang, G., Zeng, T.: Decomposition-based variational network for multi-contrast mri super-resolution and reconstruction. In: IEEE/CVF Conference on Computer Vision and Pattern Recognition. pp. 21296–21306 (2023)
9. Liu, F., Feng, L., Kijowski, R.: Mantis: model-augmented neural network with incoherent k-space sampling for efficient mr parameter mapping. Magnetic Resonance in Medicine **82**(1), 174–188 (2019)
10. Liu, X., Qiu, S., Zhou, M., Le, W., Li, Q., Wang, Y.: Wfanet-ddcl: Wavelet-based frequency attention network and dual domain consistency learning for 7t mri synthesis from 3t mri. IEEE Transactions on Circuits and Systems for Video Technology **35**(6), 5617–5632 (2025)

11. Liu, Y., et al.: Srm-net: Joint sampling and reconstruction and mapping network for accelerated 3t brain multi-parametric mr imaging. IEEE Transactions on Biomedical Engineering **72**(6), 1811–1824 (2025)
12. Liu, Z., Mao, H., Wu, C.Y., Feichtenhofer, C., Darrell, T., Xie, S.: A convnet for the 2020s. In: Proceedings of the IEEE/CVF International Conference on Computer Vision. pp. 11976–11986 (2022)
13. Mao, Y., Jiang, L., Chen, X., Li, C.: Disc-diff: Disentangled conditional diffusion model for multi-contrast mri super-resolution. In: Medical Image Computing and Computer-Assisted Intervention – MICCAI. pp. 387–397. Springer (2023)
14. Ouyang, J., Adeli, E., Pohl, K.M., Zhao, Q., Zaharchuk, G.: Representation disentanglement for multi-modal brain mri analysis. In: Information Processing in Medical Imaging. pp. 321–333. Springer (2021)
15. Qiu, Y., Zhang, H., Ma, Q., Yang, G., Lai, Z.: Multi-contrast mri reconstruction based on frequency domain separation and cross-self-attention. IEEE Access **12**, 55062–55076 (2024)
16. Ronneberger, O., Fischer, P., Brox, T.: U-net: Convolutional networks for biomedical image segmentation. In: Medical Image Computing and Computer-Assisted Intervention – MICCAI. pp. 234–241. Springer (2015)
17. Sun, K., Wang, Q., Shen, D.: Joint cross-attention network with deep modality prior for fast mri reconstruction. IEEE Transactions on Medical Imaging **43**(1), 558–569 (2024)
18. Uecker, M., et al.: Espirit—an eigenvalue approach to autocalibrating parallel mri: Where sense meets grappa. Magnetic Resonance in Medicine **71**(3), 990–1001 (2014)
19. Xiang, L., et al.: Deep-learning-based multi-modal fusion for fast mr reconstruction. IEEE Transactions on Biomedical Engineering **66**(7), 2105–2114 (2019)
20. Yan, Y., Yang, T., Jiao, C., Yang, A., Miao, J.: Iwnext: an image-wavelet domain convnext-based network for self-supervised multi-contrast mri reconstruction. Physics in Medicine & Biology **69**(8), 085005 (2024)
21. Yan, Y., et al.: Cross-modal vertical federated learning for mri reconstruction. IEEE Journal of Biomedical and Health Informatics **28**(11), 6384–6394 (2024)
22. Ye, Y., Lyu, J., Hu, Y., Zhang, Z., Xu, J., Zhang, W.: Multi-parametric mr imaging with flexible design (multiplex). Magnetic Resonance in Medicine **87**(2), 658–673 (2022)
23. Ye, Y., et al.: A multi-dimensional integration (mdi) strategy for mr t2* mapping. NMR in Biomedicine **34**(7), e4529 (2021)
24. Zhang, C., et al.: A unified model for reconstruction and r2* mapping of accelerated 7t data using the quantitative recurrent inference machine. NeuroImage **264**, 119680 (2022)